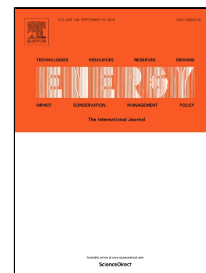# Accepted Manuscript

Slow pyrolysis of by-product lignin from wood-based ethanol production– A detailed analysis of the produced chars

Najibeh Toloue Farrokh, Hannu Suopajärvi, Olli Mattila, Kentaro Umeki, Aekjuthon Phounglamcheik, Henrik Romar, Petri Sulasalmi, Timo Fabritius

Please cite this article as: Najibeh Toloue Farrokh, Hannu Suopajärvi, Olli Mattila, Kentaro Umeki, Aekjuthon Phounglamcheik, Henrik Romar, Petri Sulasalmi, Timo Fabritius, Slow pyrolysis of by-product lignin from wood-based ethanol production– A detailed analysis of the produced chars, *Energy* (2018), doi: 10.1016/j.energy.2018.08.161

1 **Slow pyrolysis of by-product lignin from wood-based ethanol production– A detailed analysis of the**
2 **produced chars**

3 Najibeh Toloue Farrokh[a,*], Hannu Suopajärvi[a], Olli Mattila[b], Kentaro Umeki[c], Aekjuthon
4 Phounglamcheik[c], Henrik Romar[d], Petri Sulasalmi[a], Timo Fabritius[a]

5 [a] Process Metallurgy Research Unit, University of Oulu, P.O. Box 4300, FI-90014, Oulu, Finland.
6 [b] SSAB Europe Raahe steel plant.
7 [c] Energy Engineering, Division of Energy Science, Luleå University of Technology, SE-971 87, Luleå, Sweden.
8 [d] Research Unit of Sustainable Chemistry, University of Oulu, P.O. Box 3000, FI-90014, Oulu, Finland.
9
10
11

12 **Abstract:**

13 Slow pyrolysis as a method of producing a high-quality energy carrier from lignin recovered from wood-
14 based ethanol production has not been studied for co-firing or blast furnace (BF) applications up to now.
15 This paper investigates fuel characteristics, grindability, moisture uptake and the flow properties of lignin
16 chars derived from the slow pyrolysis of lignin at temperatures of 300, 500 and 650 °C (L300, L500 and
17 L650 samples respectively) at a heating rate of 5 °C min^{-1}. The lignin chars revealed a high mass and energy
18 yield in the range of 39-73% and 53-89% respectively. Pyrolysis at 500 °C or higher, yielded lignin chars
19 with low H/C and O/C ratios suitable for BF injection. Furthermore, the hydrophobicity of lignin was
20 improved tremendously after pyrolysis. Pyrolysis at high temperatures increased the sphericity of the lignin
21 char particles and caused some agglomeration in L650. Large and less spherical particles were found to be
22 a reason for high permeability, compressibility and cohesion of L300 in contrast to L500 and L650. L300
23 and L500 chars demonstrated high combustibility with low ignition and burnout temperatures. Also,
24 rheometric analysis showed that L500 has the best flow properties including low aeration energy and high
25 flow function.

26

27 **Keywords:** biomass, lignin, slow pyrolysis, combustion

28
29
30

* Corresponding author: Process Metallurgy Research Unit, University of Oulu, P.O. Box 4300, FI-90014, Oulu, Finland. Tel.: +358 469 074489
E-mail address: najibeh.tolouefarrokh@oulu.fi (N. Toloue Farrokh).

1. Introduction

Renewable energy is forecasted to play a vital role in the future energy system to reduce the accumulation of CO_2 emissions into the atmosphere. The importance of biomass in fuel applications has increased tremendously during the last decades and a similar trend is set to continue. The combustion and co-firing of biomass with fossil coal in power production has gained a lot of attention. The recent findings suggest that the thermochemical upgrading of biomass is needed to enhance the physical and chemical properties of biomass for co-firing applications [1,2]. Eddings et al. [3], carried out pilot-scale co-firing trials to evaluate the performance of co-firing pulverized coal with either raw wood, torrefied wood or bio-char. R. Perez-Jeldres et al. [4] used a computational fluid dynamics model to predict the performance of a 150MW commercial boiler co-firing pulverized coal with pine sawdust. Sahu et al. [5], studied the constraints and uncertainties associated with the use of different types of the biomass of diverse characteristics and the likely impact of the partial replacement of coal by biomass on the emission of CO_2, SO_x, NO_x.

Recently, the use of biomass as a reducing agent in iron and steelmaking applications has been proposed as an effective measure to reduce fossil CO_2 emissions [6,7]. The most efficient technology to introduce biomass into the iron and steelmaking is the replacement of pulverized coal injection to the BF with upgraded biomass fuels. In this application, a higher pyrolysis temperature is needed to produce the fuel characteristics required for BF injection [8].

A wide range of thermally upgraded woody biomasses have been studied for their applicability for co-firing and BF injection. Bergman et al. [9] studied the development of torrefaction by means of extensive parametric research, process simulations and process design for moving-bed technology. Batidziari et al. [10] provided detailed insights into state of the art prospects of the commercial utilization of torrefaction technology over time focusing on moving bed reactor while Mathieson et al. [11] considered the combustibility of different charcoal in comparison with PCI coal under simulated BF raceway conditions. Suopajärvi and Fabritius [12] also studied the production chain and the economics of biomass-based reducing agents compared to fossil-based ones. Phanphanich and Mani [1] found that the torrefaction of woody biomass enhances the chemical properties, heating value and grindability of the biomass. In the torrefaction process, in which temperatures ranged from 225 to 300 °C, the carbon content of pristine woody biomass was increased from 47.2% to 49.5–66.1%, and the heating value from 18.5 MJ/kg to 19.5–26.4 MJ/kg, depending on the torrefaction temperature. The grinding energy decreased from 237.7 to 23.9 kWh/t when wood chips were torrefied at 300 °C. Pyrolysis includes different stages. During the first stage of biomass pyrolysis, dehydration causes a shrinking of the lignocellulosic material leads to crack creations, density change and material stiffening favour grinding energy decrease [13]. Abdullah and Wu [14] reported similar enhancements in chemical and physical properties with pyrolyzed mallee eucalyptus. In slow pyrolysis, the carbon content of biochar was in the range of 82.9–85.5% when the pyrolysis temperature was 450–500 °C. Besides the chemical properties and grindability, the characteristics of fine fuel powders are important for the design of handling, storage and injection systems. Guo et al. [15] investigated the flow energy and aeration of coal and coal-sawdust blends with an FT4 Freeman powder rheometer. The basic flow energy increased with an increased rate of sawdust addition. This was because of the larger aspect ratio and the rougher surface of sawdust. Blends with sawdust additions were also insensitive to aeration, which implies that they are not suitable for dense-phase pneumatic conveying. Almendros et al. [16] evaluated the impact

of torrefaction on the flowability of the spruce powder. The basic flow and aeration energy of untreated sawdust powder decreased substantially after torrefaction at 300 °C, which implies improved flow properties. Liu et al. [17] also highlighted the impact of particle size distribution, particle shape, specific surface area, surface morphology and moisture of pulverized coal on the flowability of the powders.

The combustion properties of biomass fuels, fossil coal and their blends have been studied with thermogravimetric methods in several publications and a common finding is that biochars are more reactive in atmospheric combustion. Babich et al. [18] performed the technological and ecological assessment of blast furnace process when injecting different types of charcoal and concluded that conversion efficiency of all the tested charcoals is better or comparable with coals. Varol et al. [19] investigated the co-combustion characteristics of coal and biomass, and the synergistic effect of their various combinations on the peak temperatures and burnout times and concluded that biomass in the mixture starts to burn first and then coal follows. Park et al. [20] investigated combustion profiles of the torrefied sample and the low-temperature carbonized sample blended with coal. They verified that the fuel characteristics varied depending on the thermal treatment temperature and consequently the combustion characteristics varied. Yousaf et al. [21] investigated biochar fuels alone and blended with coal for combustion characteristics and concluded that biochar-coal co-combustion is a suitable option for its use in existing coal-fired energy generation system. assessment of combustion characteristics of blends of a coal with different biomass chars was studied by Sahu et al. [22] and the results of non-isothermal combustion studies in general depict that blends containing less than 50% biomass char are better performing as compared those with higher biomass char content.

Special emphasis should also be placed on the storage conditions of biofuels. It has been shown that the torrefaction of biomass enhances the hydrophobicity [23]. On the other hand, Gray et al. [24] reported increased water uptake of biochars with increasing pyrolysis temperature.

Even though the range of different biomasses studied is wide, the investigations of lignin in fuel applications other than burning in the Kraft recovery boilers is still quite restricted. Current developments in biorefining might lead to the further availability of lignin for materials, value-added chemicals and fuel applications [25]. Technologies such as Lignoboost [26] have been developed for Kraft-lignin extraction from black liquor in pulp production to reduce the burden on the recovery boiler. In addition, bio-ethanol production from wood-based raw materials with enzyme hydrolysis and yeast fermentation yields excessive amounts of lignin as a by-product with better chemical properties compared to Kraft-lignin. This fermented lignin has low ash, sulfur and sodium contents and is suitable for use as a raw material for the reductant production in the metallurgical industry [27]. This by-product lignin has never been studied as a fuel for power production or for BF injection. Detailed characterization of char produced from this low ash, low sulfur and low sodium lignin provides novel insights for its application in co-combustion and BF injection.

The aim of this paper is to investigate the effects of slow pyrolysis on the chemical and physical properties of lignin extracted as a by-product of wood-based ethanol production. The main objective is to evaluate the impact of slow pyrolysis temperature on mass and energy yields. Physical, chemical and morphological properties of the produced chars and their effect on grindability, moisture uptake and flow properties will be investigated and compared to pulverized coal. Finally, the combustion properties of the produced lignin chars will be discussed.

2. Materials and methods

2.1.   Materials

By-product lignin samples were received from St1 Renewable Energy Oy., which has a wood-based bio-ethanol production plant in Kajaani, Finland. In the plant bio-ethanol is produced from softwood sawdust using Cellunolix® production technology and lignin is extracted as a by-product with around 50% moisture content. This lignin was pre-dried to an approximately 4% moisture content before the slow pyrolysis experiments. Part of the lignin was in loose form, but there are also lumps of fine particles, agglomerated in the extraction process (Fig. 1). Residues of the cell wall structure of the parental wood can also be seen in the lignin samples. Pulverized coal (PC) used as a reference in this study was received from SSAB Europe Oy Raahe steel plant.

Fig. 1 By-product lignin from wood-based ethanol production.

The chemical analyses of the raw lignin, lignin chars and PC were carried out at Eurofins Ahma Oy, Oulu, Finland. Proximate analyses (ash, volatile matter, moisture) and an ultimate analysis (C, H, N, S, O) was done according to ISO 1171:2010, SFS-EN 15402:2011 and CEN/TS 15414-2:2010, SFS-EN 15407:2011, SFS-EN ISO 16994:15, SFS-EN 15408:11 and SFS-EN 15296:2011 standards. Higher and lower heating values were determined according to SFS-EN 15400:2011 standard.

2.2.   Slow pyrolysis experimental system and procedure

Slow pyrolysis experiments were conducted in a laboratory-scale batch reactor (Fig. 2). The pyrolysis system consisted of a gas tight stainless-steel tube inserted in a double chamber tube furnace (Entech ETF 75/17V), with a nitrogen cylinder, a rotameter and a pyrolysis gas treatment unit. The diameter of the reactor tube was 200 mm with a maximum bed height of around 400 mm. Pre-dried lignin was inserted into the pyrolysis reactor without any particle size classification thus, the lignin charge included fine particles and agglomerated lignin lumps. The lignin was pyrolyzed at a heating rate of 5 °C min^{-1} under N_2 (200 mL min^{-1}) up to target temperatures of 300 °C, 500 °C and 650 °C (L300, L500, L650, L=lignin). The holding time at the target temperature was eight hours. The yield of the solid products was determined by their dry basis. The moisture content of the lignin was 4 wt.%.
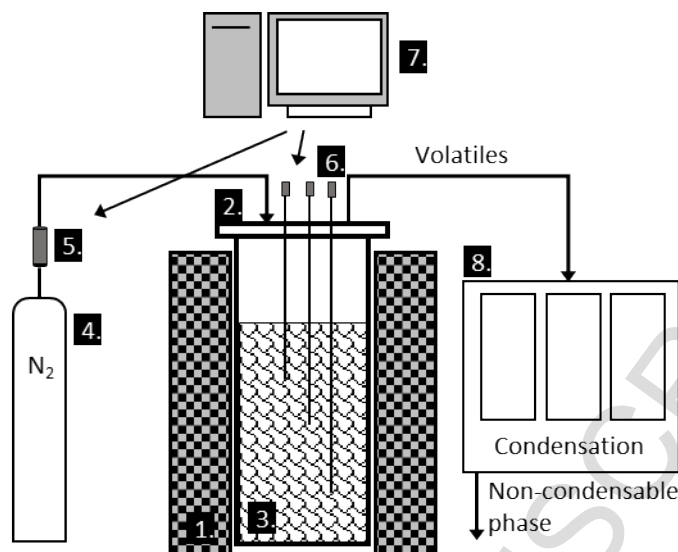
Fig. 2 A schematic picture of the slow pyrolysis system: 1. chamber furnace (Entech ETF 75/17V); 2. pyrolysis reactor; 3. biomass sample; 4. N2 cylinder; 5. gas flow controller; 6. thermocouples; 7. computer; 8. bio-oil condensers.

141 *2.3.   Grinding experiments*

142 A laboratory-scale centrifugal mill (Netzsch ZM200) was used in the grinding experiments. A 500 µm
143 grid rotor with 12 teeth and 18000 rpm rotator speed were used in the experiments. Raw lignin and
144 lignin char samples were crushed manually to a size range of 2-4 mm before the grinding test. Then the
145 samples were fed into the mill at a constant feeding rate to produce pulverized samples for subsequent
146 analyses. PC was also tested under the same grinding conditions for comparison. The grinding method
147 itself was tuned to match the size distribution of production grade coal powder. The grindability of the
148 samples was determined based on particle size distribution analysis.

149

150 *2.4.   Physico-chemical characteristics*
151 *2.4.1. Bulk and true density*

152 For a biomass to be considered a substitute for coal in iron and steel making several problems, including
153 large bulk volume, high moisture content, low heating value and energy density should be considered.
154 It is important to measure true and bulk density of chars as it helps to describe other results like moisture
155 uptake, bulk properties and rheometric properties

156 The bulk density measurements for the dried 2-4 mm sample fraction and dried pulverized samples
157 were performed by following the procedure described by Abdullah and Wu [14]. The sample was
158 poured into a cylinder with a known volume and stamped on a wooden board until the volume of the
159 cylinder content remained unchanged. The bulk density measurement was repeated three times and the
160 relative standard deviation was 1.6% on average.

161 The true density of the dried 2-4 mm sample fraction was measured using an AccuPyc 1340 Helium
162 gas pycnometer. This measurement was also repeated three times and the relative standard deviation
163 was 0.007% on average.

2.4.2. Moisture uptake

The moisture uptake of the lignin, lignin chars and PC were measured using a water immersion test. Approximately 0.5 g of the dry sample (2-4 mm fraction) was immersed in water at room temperature for two hours. Then the sample was air dried for an hour at room temperature after which the moisture content was determined [23].

2.4.3. Morphological characterization

For microscopic characterization, the sample particles were embedded in polyester resin and polished for examination under reflected light to evaluate their structure and morphology. An Olympus BX51 optical microscope equipped with a digital camera was used to evaluate the effect of the pyrolysis temperature on the char structure.

A Zeiss ULTRA plus field emission scanning electron microscope (FESEM) was also used in order to study the lignin char morphology and microstructure. A double stick carbon tape suitable for Scanning Electron Microscopy (SEM) and a gold coating were used to study the char samples.

The particle size and shape analysis of all pyrolyzed samples were performed using a CAMSIZER P4 particle analyzer for 2-4 mm fractions and pulverized samples.

2.5. Flow behavior of the fuels

The flow properties of the powders were measured with a Freeman Technology FT4 Powder Rheometer FT4 [28]. The purpose was to examine how the increase in the pyrolysis temperature affects the properties of lignin chars, which is important for powder storage in silos and flowability in pneumatic conveying lines.

The bulk properties of the powders under investigation were: the conditioned bulk density (CBD, g/ml), the tapped bulk density (50 taps) (BDtap50, g/ml), the compressibility (CPS, %), and the permeability (cm^2). The CBD was measured for the powder that had gone through gentle conditioning to create a uniform, lightly packed test sample [28]. The BDtap50 measure is the bulk density after the measurement vessel is tapped 50 times. The compressibility and the permeability tests are suited for determining the cohesiveness of the powder bed. The compressibility gives the percentage by which the volume has changed under an impact of 15 kPa at normal stress [28]. In the permeability test the pressure drop was measured across the powder bed whilst the applied normal pressure was varied and the air velocity through the bed was maintained constant at 5 mm/s [28]. The sample volume was around 300 ml and the moisture content was 1%.

Dynamic tests for the powders included the basic flow energy (BFE, mJ), aerated energy (AE, mJ) and consolidated energy (CEtap50, mJ). BFE is the energy needed to displace a powder from its stabilized and conditioned state with a given flow pattern and flow rate. The aeration energy gives the flow energy when a fluidizing gas with a velocity of 3 and 6 mm/s is introduced into the powder bed. The CEtap50 measure gives the energy needed to displace a powder sample, which has been tapped 50 times.

Shear tests for the powders included the cohesion (τ_o), the angle of internal friction (WFA, ∘) and flow function defined by Jenike (ffc). Cohesion is defined as a shear strength at zero normal stress [28]. The wall friction test provides a measurement of the sliding resistance between the powder and the surface

202 of the process equipment and is defined as the arctan of the ratio of the wall shear stress to the wall
203 under normal stress [28]. Then flow function is defined by the Jenike relation and is the ratio of the
204 major principle stress to the unconfined yield stress [28].

205 *2.6.   Thermal analysis*

206 The combustion behavior of the lignin chars and coal was studied with a Netzsch STA 449 F3 Jupiter
207 thermoanalyzer. Pulverized samples of around 5 mg were carefully spread on an alumina dish crucible
208 (17 mm diameter) and heated from 20 to 1000 °C at a heating rate of 5 °C min^{-1} under air at a flow rate
209 of 50 mL min^{-1}. Combustion parameters including the DSC peak temperature, DTG peak temperatures,
210 maximum rate of weight loss (R_{max}, %/min), initial temperature (T_i) and burn out temperature (BOT)
211 were determined for each sample. T_i is defined as the temperature, at which the derivative of the weight
212 loss curve (DTG) first reaches the value of 1 %/min. R_{max}, %/min is the maximum reactivity defined
213 from the DTG curve. BOT is the temperature at which the weight loss rate reaches the 1 %/min at the
214 terminal phase of DTG profile. The repeatability of the experiments was evaluated with duplicates.

215 **3. Results and Discussion:**

216 *3.1.   Mass and energy yield*

217 Fig. 3 shows the mass and energy yields of lignin pyrolyzed at three different temperatures along with
218 standard deviation bar which confirms repeatability of the data. The char yield decreased as the
219 temperature was raised, and the trend is similar to that of pristine wood-based biomass slow pyrolysis.
220 However, the yield of the lignin was higher compared to that of pristine biomass. For pristine woody
221 biomasses the mass yields in slow pyrolysis are usually 52–54% at 300 °C [1,29], 22–27% at 500 °C
222 and 20–26% in the temperature range of 600–700 °C [30,31], whereas the mass yield of lignin is 73.1%,
223 45.7% and 39.3% in 300 °C, 500 °C and 650 °C, respectively. The mass yield results are in agreement
224 with the thermogravimetric studies made in the slow pyrolysis heating rate region when Kraft-lignin
225 and commercial pure lignin have been studied [6,32]. There is no slow pyrolysis data for lignin extracted
226 from wood-based ethanol production in the literature up to the time of the present study. The higher
227 yield of the lignin compared to pristine biomass is because of the different decomposition behavior of
228 wood constituents; hemicellulose, cellulose and lignin. Hemicellulose decomposes in the temperature
229 range between 220 and 300 °C with a char yield of 20%, while cellulose decomposes in the temperature
230 range between 315 and 390 °C with a negligible char yield, but lignin decomposes in a broad
231 temperature range between 200 and 550 °C and with a char yield of around 50% or more [32–34]. Major
232 reasons for the higher mass yield of lignin could be that lignin has a 3D molecular structure of aromatic
233 clusters (mainly phenolic) that are ready to produce char through cross-linking reactions [35]. Sharma
234 et al. [36] also observed that char yield in pyrolysis decreased rapidly with an increase in temperature.
235 They studied lignin char and its reactivity towards the formation of polycyclic aromatic hydrocarbons
236 (PAHs) by many different chemical bond analysis methods. They described their observation by the
237 fact that the aromaticity and the carbonaceous nature of the char increased with temperature and the
238 char lost hydrogen and oxygen preferentially as the temperature increased. They related the decrease in
239 the O/C ratio to some decarboxylation together with dehydration. They also showed that chars lost both
240 hydroxyl and aliphatic groups as the pyrolysis temperature increased and the aromatic character
241 increased rapidly above 450 °C.

The high mass yield also resulted in a high energy yield, which ranged from 53% to 89% depending on the slow pyrolysis temperature, calculated from higher heating values and dry basis. The energy yield of lignin is high, compared to energy yields of biochar from the slow pyrolysis of pristine woody biomass, which are usually 50% at 300 °C, 40% at 500 °C and 35% at 650 °C [8].
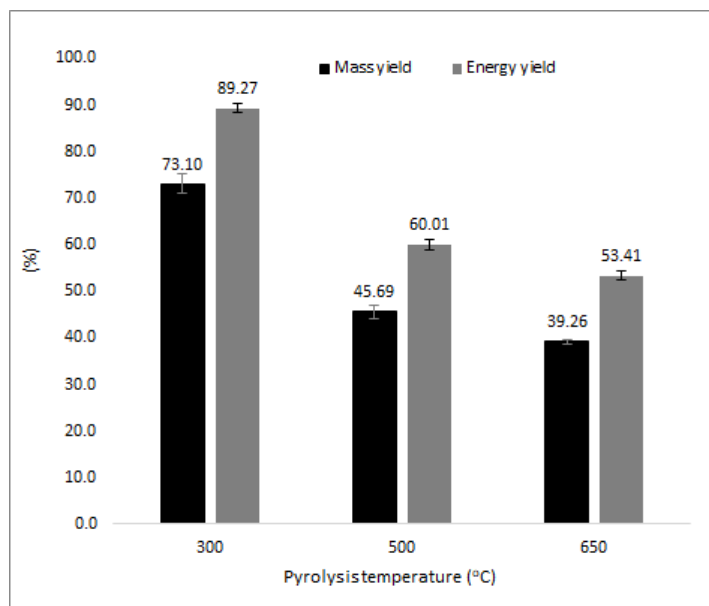

Fig. 3 The effect of temperature on mass and energy yields of pyrolyzed lignin.

As stated in section 2.2, raw lignin was fed into the pyrolysis chamber without any particle size classification. It is known that the amount and nature of the products released during pyrolysis are influenced by the initial particle size [37,38]. It should be noted that in this study, residence time of the raw lignin in the reactor was set to 8 hours to make sure the particle mass stops changing and insufficient heat transfer does not affect pyrolysis of bigger particles. This way the effect of particle size on lignin pyrolysis and mass/energy yield can be neglected. Furthermore, slow pyrolysis experiments with a low heating rate of 5 °C min^{-1} minimize the possible effects of initial particle size of lignin on the characteristics of obtained chars.

3.2.   Fuel characteristics

Table 1 presents the data of proximate, ultimate and heating value analyses for raw lignin, pyrolyzed lignin and PC. The heating value of the lignin (25.2 MJ/kg db) is high compared to pristine wood-based biomasses such as pine wood (19 MJ/kg db), wheat straw (16 MJ/kg db) and algae (14 MJ/kg db) [39] and could possibly be used in co-firing applications without any thermal treatment. However, for BF injection, the high share of oxygen and volatiles, and low share of fixed carbon in the material inhibits its applicability. It can be seen in the Table 1 that by increasing the pyrolysis temperature, the share of fixed carbon increased and the share of oxygen and volatiles decreased, as expected. This analysis also showed that lignin and lignin chars have substantially lower ash, sulfur and nitrogen contents compared to the reference PC.

As Li et. al explained [31], pyrolysis breaks weak bonds to release volatiles and gases, and subsequent rearrangement reactions strengthen the carbon matrix, resulting in a bio-char with high fixed carbon content and low volatile content. Volatiles are released by the breaking of chemical bonds. Increased

269 temperature supplies more energy to the system, resulting in more broken bonds. So, higher pyrolysis
270 temperatures diminished the H/C ratio due to the enrichment of carbon in the charred material and the
271 release of hydrogen through the volatile products and moisture.

272 **Table 1** Physico-chemical properties of the fuels.

Materials	MC* (%, wb)	VM* (%, db)	Ash (%, db)	FC* (%, db)	C (%, db)	H (%, db)	N (%, db)	S (%, db)	O (%, db)	HHV* (MJ/kg, db)
Lignin	3.4	74.0	0.3	26.1	61.3	6.23	0.70	0.087	31.4	25.22
L300	< 1.0	41.0	0.5	59.2	75.3	5.14	0.97	0.101	18.0	30.18
L500	< 1.0	18.0	0.7	83	85.9	3.56	1.23	0.121	8.6	33.12
L650	< 1.0	5.1	0.9	94.0	93.7	2.05	1.33	0.115	1.9	34.31
PC	< 1.0	21.4	10.1	68,4	78.3	4.17	2.06	0.221	5.1	30.53

MC= Moisture Content, VM= Volatile Materials, FC= Fixed Carbon, HHV= High Heating Value.

273

274 The H/C and O/C ratios of lignin and lignin chars are depicted in the Van Krevelen diagram in Fig. 4
275 together with PC and chars from pinewood sawdust [31]. The required properties for fuels are dependent
276 on their application. In the case of BF injection, a low O/C is required for an efficient process [8]. A
277 slow pyrolysis temperature of 500 °C is low and falls within the desired range which is enough to
278 produce a high-quality biochar for BF injection from lignin, whereas in case of pristine pine, the slow
279 pyrolysis temperature should be higher [31]. For co-firing applications, the mild carbonization of lignin
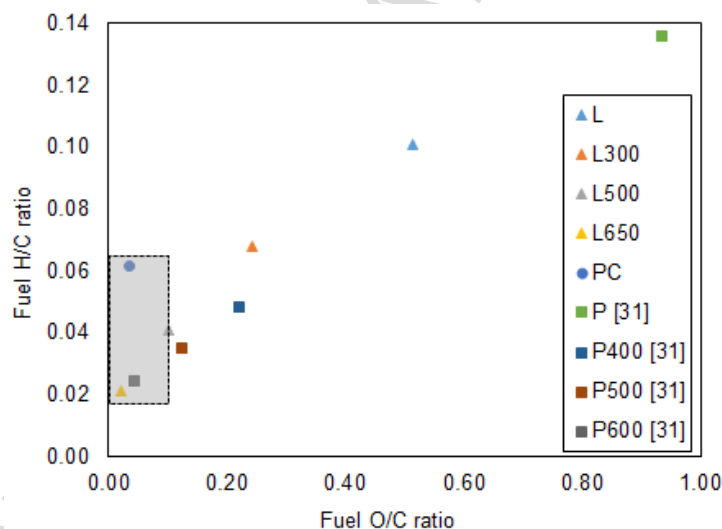280 occurs at 300 °C, or lower, and could lead to adequate fuel properties [1].

281

282 **Fig. 4** Van Krevelen diagram. (L: Lignin, P: pinewood sawdust, PC: pulverized coal, numbers after the letter is the temperature in which
283 each sample is pyrolyzed)

284 *3.3.   Physical characterization*
285 *3.3.1. Density*

286 Bulk and true densities of the 2-4 mm fraction lignin, lignin chars and PC and bulk density of pulverized
287 samples are shown in Table 2. It can be seen that the bulk and true densities of 2-4 mm lignin samples
288 increased with an increasing pyrolysis temperature. The increase in the bulk density was 10.4% from
289 the L300 to the L650 samples. The bulk density of the lignin chars is 52.8–57.2% of the bulk density
290 of PC. Abdullah and Wu [14] did not find a relation between pyrolysis temperature and bulk density

for unground charcoals produced from mallee eucalyptus at different slow pyrolysis temperatures (300-500 °C). It seems that bulk density increased with increasing temperature in accordance to increase in denser components like carbon and ash and decreasing in light components including H and O. Also, the resulting products pyrolyzed at higher temperatures seemed to obtain structural shrinkage, causing higher bulk density. During pyrolysis, a significant loss of volatile and condensable compounds from the biomass increases the true density, leading to the shrinkage of pyrolyzed matrices to form highly carbonaceous materials. Furthermore, the devolatilization may collapse the void volume in the biomass char to raise the true density [40].

Bulk density measurements conducted for pulverized lignin chars showed an even stronger dependency on the pyrolysis temperature. The bulk density of the L300 samples was 488 kg/m^3 whereas the bulk density of the L650 samples was 737 kg/m^3, which is over a 51% increase and quite close to the bulk density of PC. Abdullah & Wu [14] reported a similar increase in the bulk density of pulverized charcoals with increasing temperatures. They also showed that the bulk densities of biochar samples after grinding was 600-700 kg/m3, which was a significant improvement from the unground biochars (~300 kg/m3). The lower bulk density of lump form biochars requires special consideration when designing efficient supply chains and storage systems for lignin and lignin chars. The comparable bulk density of the pulverized lignin chars (L500 and L650) to the bulk density of PC is a promising result in terms of biofuel handling and possible blending with fossil coals. The bulk densities reported here present the maximum range of values, since the materials were packed by extensive tapping.

Comparing the true density and bulk density of 2-4 mm lignin chars confirms the effect of open pore and voids in the structure of the produced lignin chars resulting in quite low bulk densities. This observation can help to describe moisture uptake, bulk properties and the flowability of the samples [41].

Table 2 Bulk density of the 2-4 and pulverized fraction and true density of 2-4 mm fraction.

	Bulk density, 2-4 mm fraction (kg/m^3)	Standard deviation	Bulk density, pulverized fraction (kg/m^3)	Standard deviation	True density, 2-4 mm fraction (g/cm^3)	Standard deviation
Lignin	351.3	9.0	478.5	24.9	1.39	0.001
L300	339.5	3.8	487.7	6.7	1.36	0.001
L500	342.8	0.4	668.3	4.3	1.74	0.094
L650	374.9	0.7	737.0	2.1	1.97	0.115
PC	794.6	2.0	835.3	1.8	1.47	0.008

3.3.2. Grindability

A particle size distribution analysis was used to compare the grindability of the samples in this study. Biomasses usually have poor grindability because of their bulky and fibrous nature. The grindability of the raw biomasses can be substantially enhanced by torrefaction or slow pyrolysis [13,14]. The grindability of lignin lumps has not been reported earlier. As all the samples had almost similar particle sizes before grinding in the centrifugal mill, the grindability of the materials could be evaluated from the particle size distribution. The smaller the particles become in the grinding; the better the grindability [14]. Fig. 5 a-b shows the cumulative particle size distribution and particle size distribution of ground raw lignin, lignin chars and PC. In addition, Table 3 provides numerical cumulative particle size data for the samples. It can be seen that the grindability of all the pyrolyzed lignins was quite close to that

326 of PC. There was an increase in the particle sizes between the raw state and the L300 samples (Table 3
327 and Fig. 5). Then, the particle sizes decreased slightly from the L300 to the L500 samples. Again,
328 temperature increases led to an increase of the mean and d50 in the L650 samples compared to the L500
329 samples, which is visible in Figure 5 and Table 3. However, the D90 results showed a continuous
330 increase in the particle size with an increasing pyrolysis temperature. The L650 samples had the worst
331 grindability, which can be seen in the higher share of larger particles. Raw lignin itself has a small
332 particle size and the raw lignin lumps break and grind easily. It seems that the increase in the pyrolysis
333 temperature resulted in the opposite grindability behavior in the case of by-product lignin compared to
334 raw woody biomasses [23]. This may be a result of stronger agglomeration and packing of the lignin
335 structure.

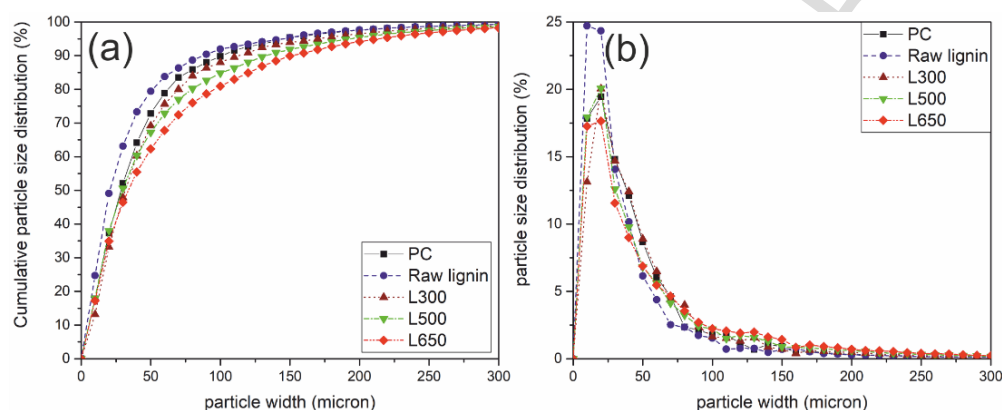**Fig. 5** a) Cumulative particle size distribution and b) particle size distribution of pulverized raw lignin, lignin chars and coal.

Table 3 Properties of particle size distribution of lignin and coal samples.

	Mean (μm)	d_{10} (μm)	d_{50} (μm)	d_{90} (μm)
Lignin	37.27	6.31	19.90	84.79
L300	55.37	8.86	33.99	128.98
L500	53.95	7.26	29.7	135.14
L650	59.28	7.23	32.97	150.49
PC	45.85	7.14	28.935	106.14

339 ### 3.3.3. *Moisture uptake*

340 The moisture adsorption properties of biomass-based fuels are important for proper handling and
341 storage solutions. PCs are usually stored in outside storage areas, since their moisture uptake is quite
342 low. The results of water immersion tests are depicted in Fig. 6. Comparing the moisture uptake of raw
343 and pyrolyzed lignin, it can be seen that pyrolysis played very important role in reducing moisture
344 uptake. It can also be noted that the moisture uptake of the PC was very low. In the results, there is a
345 clear trend in the moisture uptake development in lignin chars with an increasing pyrolysis temperature.
346 The higher the pyrolysis temperature, the higher the moisture uptake but still quite much lower than
347 that of raw lignin. Similar findings have been reported for pristine wood biochars by Gray et al [24]
348 who found that water uptake of biochar was dependent on the feedstock type (which controls the
349 residual macroporosity) and the production temperature (which controls the hydrophobicity).
350 Hydrophobicity in biochars decreases with an increasing production temperature and this may be due
351 to less hydrophobic aliphatic functional groups which are volatilized and lost at higher production
352 temperatures [24,42,43]. It can be concluded that thermal treatment is a method that can solve the
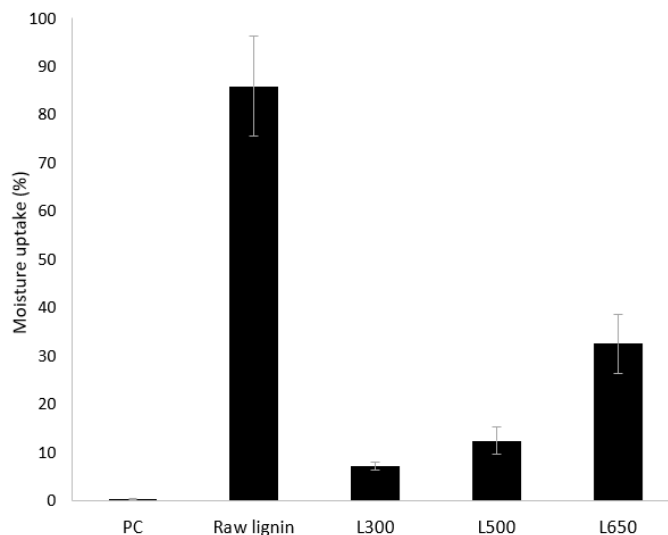353 problem of moisture adsorption by biomass during handling and storage [44].

Fig. 6 Moisture uptake in water immersion test for 2-4 mm samples.

3.4.   Morphological changes to the structure of pyrolyzed lignin
3.4.1.   Optical and scanning electron microscopy

The microstructures of pyrolyzed lignin samples at 300, 500 and 650 °C are depicted in Fig. 7. In the prepared section of samples, the white phase represents lignin. All the pyrolyzed lignin contains a matrix of linked particles. In the L300 samples the substrate network was denser with fewer voids while the L500 samples showed a narrower particle network and smaller colonies of lignin particles. Again, in the L650 samples, there were wider areas of agglomerates.

Pyrolysis and the release of volatile materials usually results in a more open structure in pyrolyzed samples containing a mainly wood structure [45,46], but for the lignin samples, as mentioned earlier in the particle size distribution results, it was different.

A slight agglomeration of fines occurred in the char samples pyrolyzed at high temperatures. This agglomeration can be seen in the SEM images of the lignin chars in Fig. 8. In this picture, the L500 samples have smaller particles compared to the L300 samples, while the L650 samples confirmed result which was observed in the particle size analysis in Fig. 5 and Table 3.

In lignocellulosic biomass, lignin is a three-dimensional network of polymers with extensive intra and intermolecular bonds that embed cellulose and hemicellulose fibers within it. During pyrolysis, the polymer structure of the lignin undergoes degradation stages including softening (at less than 300 °C), bond breakage (starting at about 300) and solidification (cross-linking at around 400 °C and higher) [47]. Based on these transformation stages, the L300 samples were affected by the softening and adherence of small particles. In the L500 samples the release of significant amounts of volatile materials led to a narrow network of particles containing many voids. Finally, in the L650 samples, the solidification stage led to a higher degree of cross-linking and widely agglomerated particles.
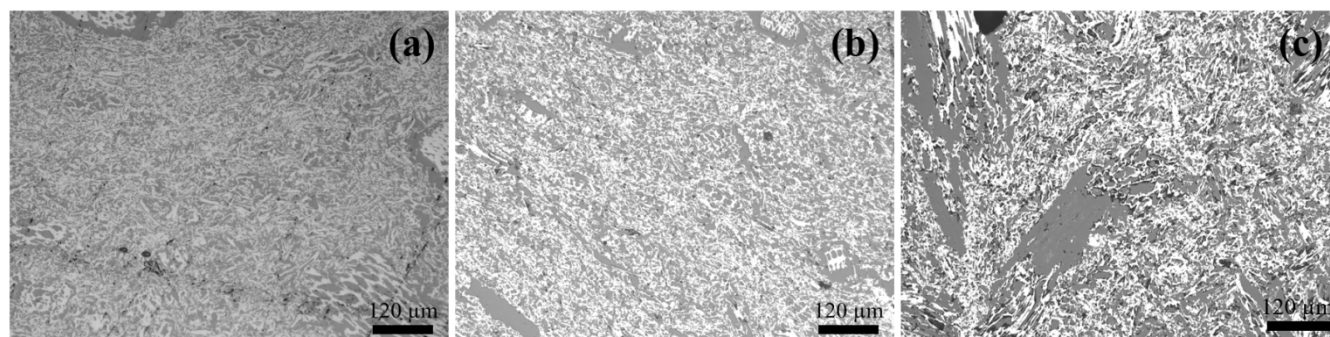
379

380

Fig. 7 Optical microscope images of 2-4mm lignin samples: (a) L300, (b) L500, (c) L650, 100X magnification.
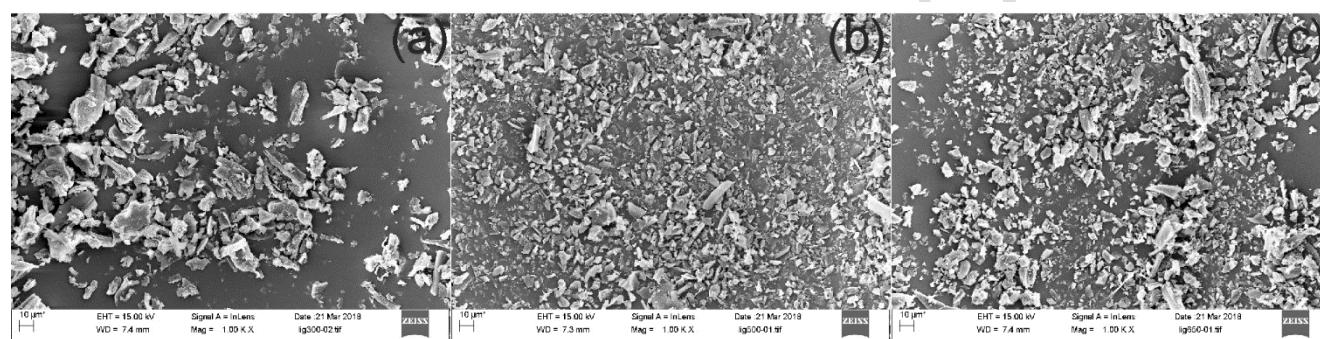

382

383

Fig. 8 SEM of powder lignin samples: (a) L300, (b)L500, (c)L650, 1000X magnification.

3.4.2. Particle shape analysis

Among the different changes that pyrolysis brings to lignin, particle shape changes can also be considered. The effects of particle shapes on the rheological properties of fuels have been discussed in many papers [15,16]. Fig. 9 illustrates the sphericity (a) and aspect ratio (b) of the samples measured in every size fraction. As expected, raw lignin particles were highly irregular in shape but after pyrolysis the shape of the lignin chars were more spherical and similar to PC. With an average sphericity of 0.806, the L300 samples showed the lowest sphericity compared to 0.818 for the L500 samples and 0.821 for the L650 samples. Similar findings were observed in the measured aspect ratios of lignin, lignin char and PC samples.
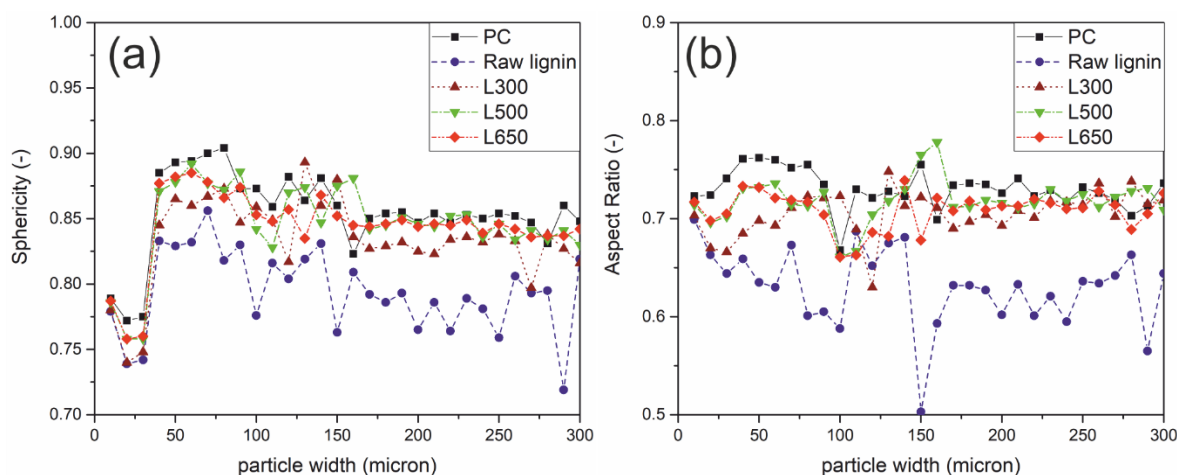
Fig. 9 Particle shape analysis a) sphericity and b) aspect ratio of raw lignin, lignin chars and PC.

3.5.   *Flow and transport properties*

3.5.1. *Bulk properties*

Conditioned and tapped bulk densities of the pulverized samples are shown in Fig. 10. The densities measured using the FT4 Freeman powder rheometer are considerably lower compared to the ones presented in Table 2. These density results provide a better understanding of the powder packing tendency in the conditions found in a pneumatic conveying system. It can be seen that the conditioned bulk density of the lignin chars increased with the pyrolysis temperature, almost reaching the CBD of the PC. The bulk density of the pulverized samples increased after tapping 50 times, but the increase was rather modest.
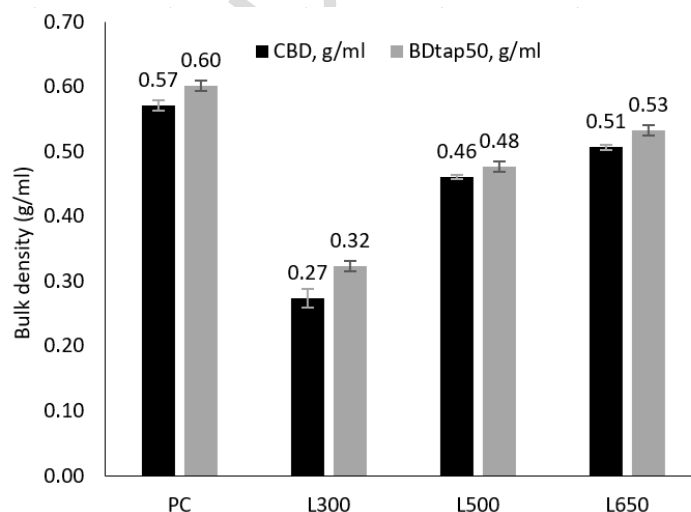

Fig. 10 Conditioned and tapped bulk density.

The compressibility of the pulverized samples is shown in Fig. 11 a. This shows that the compressibility of the L300 samples was the highest whereas the compressibility of the L500 and L650 samples was close to the compressibility of PC. The high compressibility of the L300 samples indicates a higher percentage of void space inside the material bed. This was also evident in the lower bulk density of the

conditioned powder mentioned earlier. Higher compressibility and a lower bulk density could result in less efficient particle packing of the L300 samples which is probably due to their irregular shape (lower sphericity).

The permeability of the powder samples was calculated based on the pressure drop across the powder bed under normal stress of 15 kPa. Permeability in the case of the L300 char samples was significantly higher (Fig. 11 b) which means more cohesive behavior of the L300 samples which may be due to their low sphericity which makes a low-density porous bed. The permeability of the L500 and L650 char samples were quite similar and close to that of PC.

In pneumatic transfer lines where particles are separated and carried by the carrying gas, the effectiveness of pneumatic transfer can be estimated from material permeability values. The higher the permeability the bigger share of carrying gas will pass through the material bed without transferring materials. Effective pneumatic transfer favors low or moderate permeability values.
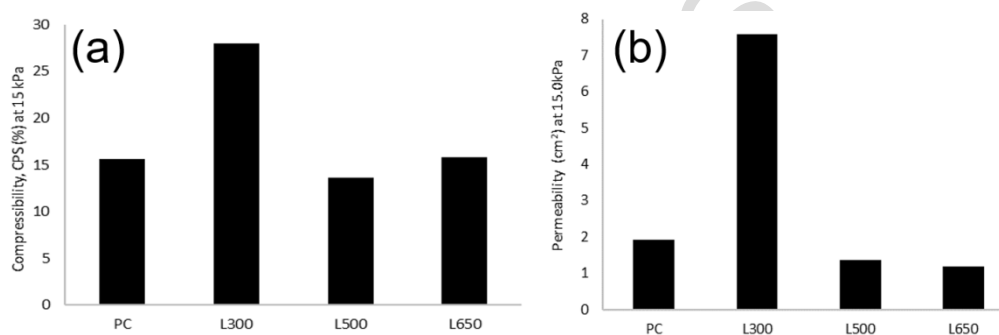

Fig. 11 Bulk properties of lignin chars and coal a) Compressibility and b) permeability.

3.5.2. Dynamic properties

Basic flow energy (BFE) and aeration energy (AE) results can be used as indications of the dynamic flow properties of the lignin chars and PC and these are depicted in Fig. 12 (a-b). From the BFE bar diagram in Fig. 12 a, it can be observed that the basic flow energy of the lignin chars did not change considerably with the increasing pyrolysis temperature and was similar to the BFE for the PC. To be more precise, the L300 samples displayed the lowest BFE compared to the rest of the samples. This is mainly due to the lower bulk density and lower aspect ratio of the L300 samples (Fig 11, Fig. 9 b) [15]. In a BFE test of a low bulk density powder less energy is required for the blade to pass through the powder bed, and a low aspect ratio caused the easier movement of the blade through the open and randomly packed bed of the L300 sample.

In addition, as depicted in Fig. 12 b, the aerated energy (AE) index test shows higher AE at different gas velocities for the L300 samples, which is most likely affected by the irregular particle shape. The high cohesion of the L300 powder which is reflected in its low bulk density and high permeability is a reason for the higher aeration energy of the L300 samples. It means that higher energy is required to make the L300 powder flow when it is aerated with gas as compared to other samples. Aeration itself helps the flowability as it can be seen in the reduction of the BFE of the L300 samples, but the higher cohesion of this powder is better understood through the AE results.

442   The L500 and L650 samples displayed lower AE levels, which were even lower for PC, it may highlight
443   the effect of their broad particle size distribution [48]. The lower aeration energy values for the L500
444   and L650 samples might be considered very good from a technical perspective. This means that the
445   particles will flow easily with a lower tendency to cause blockages during pneumatic conveying or
446   injection into a BF [49]. However, it should be kept in mind that very high permeability values of
447   powder would cause conveying gases to pass through the powder without moving it in the pipeline.
448   Furthermore, very low permeability values would prevent fluidization gases from reducing the energy
449   demand to maintain the flow and might cause problems in silo bottoms. "Moderate" permeability values
450   are considered the best, but the limits of the permeability values are hard to determine. For example, a
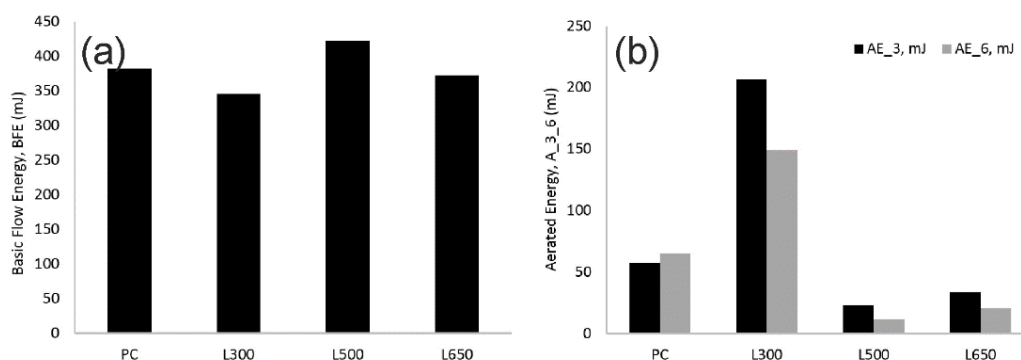451   BFE of 600 mJ and above indicates pneumatic conveying problems in case of PC [50].

452

453   **Fig. 12** Dynamic properties of lignin chars and coal a) BFE, b) AE3 and AE6.

454   *3.5.3. Shear properties*

455   Fig. 13 indicates the cohesion (C), wall friction angle and flow function (FF) index for lignin chars
456   obtained at different pyrolysis temperatures. The results show that increasing the pyrolysis temperature
457   reduced the cohesion of the chars and pyrolyzing at 500 °C made the lignin char the least cohesive of
458   all. The pyrolysis temperature had no sharp effect on the wall friction angle, and the sliding resistance
459   of all lignin chars was in the range of 18-20 º.

460   According to the FF index, powder materials are classified based on their flow properties. As the
461   measured FF values illustrate in Fig. 13 c, the L300 and L650 samples displayed an easy flowing
462   properties but the L500 samples were the best and were classified as a free flowing powder [17]. Again,
463   it is worth mentioning that extreme free flowing properties of a powder may not be considered desirable
464   as a free flowing powder can flow through the dosing screw like a liquid and cause powder leakage in
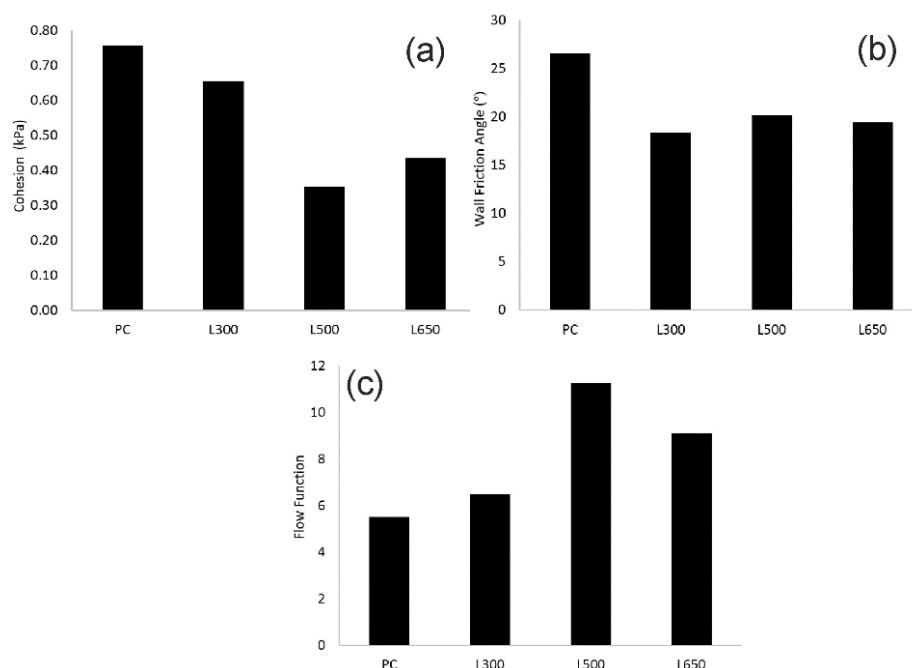465   slide gate valves or ball valves [50].

466

467 **Fig. 13** Shear properties of lignin chars and coal a) cohesion, b) wall friction angle and c) flow function.

468 *3.6. Combustibility*

469 Fig. 14 reports the TG-DTG profiles illustrating the combustion of the PC and lignin chars pyrolyzed
470 at different temperatures. The corresponding temperatures of ignition (T_i), DSC peak, DTG peak, burn
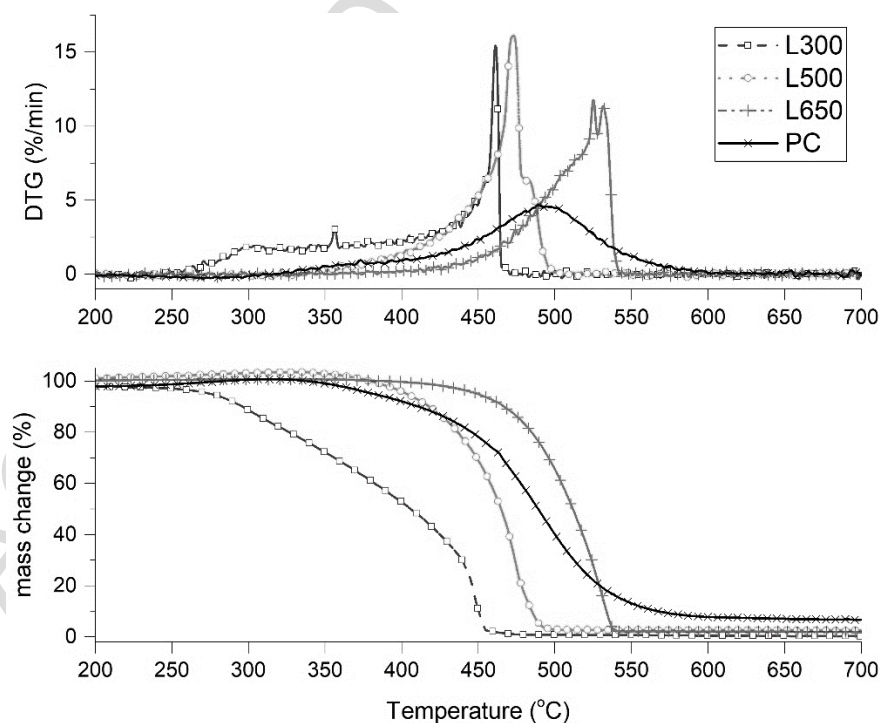471 out temperature (BOT) and the maximum rate of weight loss, R_{max}, are as displayed in Table 4.

472

473 **Fig. 14** TG and DTG profiles of coal and char combustion in the air (heating rate 5 °C min^{-1}).

474 The DTG peak of lignin chars shifted to higher temperature indicating the drifting of the combustion
475 zone, and this effect was quite noticeable with an increase in pyrolysis temperature from 300 to 650 °C.

476 **Table 4** Combustion properties of coal and lignin chars.

	T_i (°C)	DSC (°C)	DTG (°C)	R_{max} (%/min)	BOT (°C)
L300	286	462	461	15.44	465
L500	390	474	473	16.07	493
L650	448	531	525	11.77	539
PC	410	493	488	4.6	553

477

478 Because of a higher volatile material content, thermal decomposition of the L300 samples occurred in
479 a wide temperature range starting at about 300 °C and the weight loss is attributed to release of volatile
480 materials, thermal degradation of the lignin and small amount of cellulose and hemicellulose
481 components, which are present as residues in the lignin samples [20]. However, the L500 samples
482 behaved more like PC with their major combustion zone (~76% weight loss) in a single zone with a
483 temperature range of 400–500 °C and a combustibility comparable to PC. A higher degree of
484 devolatilization in pyrolysis at higher temperatures leading to lower quantities of volatile materials and
485 a higher fixed carbon content in chars might be the reason for the lower weight loss of the L500 samples
486 in comparison to the L300 samples during char combustion [21]. Pyrolysis at higher temperatures leaves
487 a char with ordered crystalline structure with low reactivity and this was evident in the late combustion
488 and high Ti of the L650 samples [51]. Therefore, there might be some restriction on using L650 in BF
489 since high combustibility is essential for a fuel in pulverized coal injection. In this case, increased O_2
490 enrichment might be a solution [52,53].

491 The combustion profile and relevant temperatures of lignin chars revealed a reduction in the peak
492 temperature, T_i and BOT by reducing the pyrolysis temperature of the chars indicating higher
493 combustibility. This can be attributed to the combined effect of the volatile combustion of the highly
494 volatile lignin char and biomass pyrolysis [52]. Volatiles released from lignin char would enhance the
495 devolatilization of the rest of the material. This early ignition of biomass is a key factor in the earlier
496 completion of volatile combustion and the consequential improvement in particle burnout as it is noted
497 in a study by Abbas et al. on lignin char combustion [54].

498 **4. Conclusions**

499 The slow pyrolysis of lignin extracted as a by-product of wood-based ethanol production was studied
500 to examine the extensive properties of lignin chars produced at three different temperatures of 300, 500
501 and 650 °C. Results showed that slow pyrolysis improves physical and chemical properties of lignin
502 with the best results for the lignin char obtained in pyrolysis at 500 °C. The main findings are
503 summarized as follows.

504 • The mass and energy yields of lignin were high, though they were reduced with increasing pyrolysis
505 temperature. The heating values of lignin and lignin chars were close to that of PC. In the case of
506 BF injection, pyrolysis at 500 °C was enough to result in an adequate chemical analysis and O/C
507 and H/C ratios for lignin.

- The pyrolysis of lignin improved its hydrophobicity tremendously while the water uptake of lignin chars produced at higher temperatures was higher due to severe devolatilization and as reported by other researchers, is due to less hydrophobic aliphatic functional groups.
- The results of particle size distribution analysis and SEM of the samples revealed that although some agglomeration occurred in the L300 and L650 samples, the grindability of the pyrolyzed lignin chars especially the L500 samples was very good and comparable to that of PC. In addition, of all samples studied, L500 powder which was more spherical with a higher bulk density displayed lower compressibility and permeability along with lower cohesion and aeration energy. The L500 char was also categorized as a free-flowing powder based on its flow function index.
- Thermogravimetric indices like T_i and BOT, DTG and DSC peak temperatures for combustion analysis revealed that the combustibility of lignin chars decreased as the temperature of pyrolysis increased but still it was better for L300 and L500 samples than PC.

Acknowledgments

References

[1] M. Phanphanich, S. Mani, Impact of torrefaction on the grindability and fuel characteristics of forest biomass, Bioresour. Technol. 102 (2011) 1246–1253. doi:10.1016/j.biortech.2010.08.028.

[2] W.H. Chen, P.C. Kuo, A study on torrefied of various biomass materials and its impact on lignocellulosic structure simulated by a thermogravimetry, Energy. 35 (2010) 2580–2586. doi:10.1016/j.energy.2010.02.054.

[3] E.G. Eddings, D. McAvoy, R.L. Coates, Co-firing of pulverized coal with Pinion Pine/Juniper wood in raw, torrefied and pyrolyzed forms, Fuel Process. Technol. 161 (2017) 273–282. doi:10.1016/j.fuproc.2015.11.020.

[4] R. Perez-Jeldres, P. Cornejo, M. Flores, A. Gordon, X. Garcia, A modeling approach to co-firing biomass/coal blends in pulverized coal utility boilers: Synergistic effects and emissions profiles, Energy. 120 (2017) 663–674. doi:10.1016/j.energy.2016.11.116.

[5] S.G. Sahu, N. Chakraborty, P. Sarkar, Coal-biomass co-combustion: An overview, Renew. Sustain. Energy Rev. 39 (2014) 575–586. doi:10.1016/j.rser.2014.07.106.

[6] H. Suopajärvi, A. Kemppainen, J. Haapakangas, T. Fabritius, Extensive review of the opportunities to use biomass-based fuels in iron and steelmaking processes, J. Clean. Prod. 148 (2017) 709–734. doi:10.1016/j.jclepro.2017.02.029.

[7] E. Mousa, C. Wang, J. Riesbeck, M. Larsson, Biomass applications in iron and steel industry: An overview of challenges and opportunities, Renew. Sustain. Energy Rev. 65 (2016) 1247–1266. doi:10.1016/j.rser.2016.07.061.

[8] H. Suopajärvi, K. Umeki, E. Mousa, A. Hedayati, H. Romar, A. Kemppainen, C. Wang, A. Phounglamcheik, S. Tuomikoski, N. Norberg, A. Andefors, M. Öhman, U. Lassi, T. Fabritius, Use of

biomass in integrated steelmaking – Status quo, future needs and comparison to other low-CO2 steel production technologies, Appl. Energy. 213 (2018) 384–407. doi:10.1016/j.apenergy.2018.01.060.

[9] P.C. a Bergman, a R. Boersma, R.W.R. Zwart, J.H. a Kiel, Torrefaction for biomass co-firing in existing coal-fired power stations, 2005. doi:ECN-C--05-013.

[10] B. Batidzirai, A.P.R. Mignot, W.B. Schakel, H.M. Junginger, A.P.C. Faaij, Biomass torrefaction technology: Techno-economic status and future prospects, Energy. 62 (2013) 196–214. doi:10.1016/j.energy.2013.09.035.

[11] J.G. Mathieson, H. Rogers, M. a. Somerville, S. Jahanshahi, Reducing Net CO2 Emissions Using Charcoal as a Blast Furnace Tuyere Injectant, ISIJ Int. 52 (2012) 1489–1496. doi:10.2355/isijinternational.52.1489.

[12] H. Suopajärvi, T. Fabritius, Towards more sustainable ironmaking-an analysis of energy wood availability in finland and the economics of charcoal production, Sustain. 5 (2013) 1188–1207. doi:10.3390/su5031188.

[13] V. Repellin, A. Govin, M. Rolland, R. Guyonnet, Energy requirement for fine grinding of torrefied wood, Biomass and Bioenergy. 34 (2010) 923–930. doi:10.1016/j.biombioe.2010.01.039.

[14] H. Abdullah, H. Wu, Biochar as a fuel: 1. Properties and grindability of biochars produced from the pyrolysis of mallee wood under slow-heating conditions, Energy and Fuels. 23 (2009) 4174–4181. doi:10.1021/ef900494t.

[15] Z. Guo, X. Chen, Y. Xu, H. Liu, Study of flow characteristics of biomass and biomass-coal blends, Fuel. 141 (2015) 207–213. doi:10.1016/j.fuel.2014.10.062.

[16] M. Almendros, O. Bonnefoy, A. Govin, W. Nastoll, M. Almendros, O. Bonnefoy, A. Govin, W. Nastoll, E. Sanz, Changes on wood powder morphology and flowability due to thermal pretreatment, Récents Progrès En Génie Des Procédés. 101 (2011).

[17] Y. Liu, X. Guo, H. Lu, X. Gong, An investigation of the effect of particle size on the flow behavior of pulverized coal, Procedia Eng. 102 (2015) 698–713. doi:10.1016/j.proeng.2015.01.170.

[18] A. Babich, D. Senk, M. Fernandez, Charcoal Behaviour by Its Injection into the Modern Blast Furnace, ISIJ Int. 50 (2010) 81–88. doi:https://doi.org/10.2355/isijinternational.50.81.

[19] M. Varol, A.T. Atimtay, B. Bay, H. Olgun, Investigation of co-combustion characteristics of low quality lignite coals and biomass with thermogravimetric analysis, Thermochim. Acta. 510 (2010) 195–201. doi:10.1016/j.tca.2010.07.014.

[20] S.W. Park, C.H. Jang, K.R. Baek, J.K. Yang, Torrefaction and low-temperature carbonization of woody biomass: Evaluation of fuel characteristics of the products, Energy. 45 (2012) 676–685. doi:10.1016/j.energy.2012.07.024.

[21] B. Yousaf, G. Liu, Q. Abbas, R. Wang, M. Ubaid Ali, H. Ullah, R. Liu, C. Zhou, Systematic investigation on combustion characteristics and emission-reduction mechanism of potentially toxic elements in biomass- and biochar-coal co-combustion systems, Appl. Energy. 208 (2017) 142–157. doi:10.1016/j.apenergy.2017.10.059.

[22] S.G. Sahu, P. Sarkar, N. Chakraborty, A.K. Adak, Thermogravimetric assessment of combustion characteristics of blends of a coal with different biomass chars, Fuel Process. Technol. 91 (2010) 369–378. doi:10.1016/j.fuproc.2009.12.001.

[23] R.H.H. Ibrahim, L.I. Darvell, J.M. Jones, A. Williams, Physicochemical characterisation of torrefied biomass, J. Anal. Appl. Pyrolysis. 103 (2013) 21–30. doi:10.1016/j.jaap.2012.10.004.

[24] M. Gray, M.G. Johnson, M.I. Dragila, M. Kleber, Water uptake in biochars: The roles of porosity and

589   hydrophobicity, Biomass and Bioenergy. 61 (2014) 196–205. doi:10.1016/j.biombioe.2013.12.010.

590   [25]   M.D. Cannatelli, A.J. Ragauskas, Conversion of lignin into value-added materials and chemicals via
591   laccase-assisted copolymerization, Appl. Microbiol. Biotechnol. 100 (2016) 8685–8691.
592   doi:10.1007/s00253-016-7820-1.

593   [26]   P. Tomani, The lignoboost process, Cellul. Chem. Technol. 44 (2010) 53–58.
594   http://www.scopus.com/inward/record.url?eid=2-s2.0-77954731901&partnerID=tZOtx3y1.

595   [27]   H. Suopajärvi, E. Dahl, A. Kemppainen, S. Gornostayev, A. Koskela, T. Fabritius, Effect of charcoal and
596   Kraft-lignin addition on coke compression strength and reactivity, Energies. 10 (2017).
597   doi:10.3390/en10111850.

598   [28]   R. Freeman, Measuring the flow properties of consolidated, conditioned and aerated powders - A
599   comparative study using a powder rheometer and a rotational shear cell, Powder Technol. 174 (2007) 25–
600   33. doi:10.1016/j.powtec.2006.10.016.

601   [29]   P.T. Williams, S. Besler, The Influence of Temperature and Heating Rate on the Slow Pyrolysis of Biomass,
602   Renew. Energy. 7 (1996) 233–250. doi:10.1016/0960-1481(96)00006-7.

603   [30]   V. Chiodo, G. Zafarana, S. Maisano, S. Freni, F. Urbani, Pyrolysis of different biomass: Direct comparison
604   among Posidonia Oceanica, Lacustrine Alga and White-Pine, Fuel. 164 (2016) 220–227.
605   doi:10.1016/j.fuel.2015.09.093.

606   [31]   A. Li, H. Liu, H. Wang, H. Xu, L. Jin, J. Liu, Effects of Temperature and Heating Rate on the
607   Characteristics of Molded Bio-char, BioResources. 11 (2016) 3259–3274. doi:10.15376/biores.11.2.3259-
608   3274.

609   [32]   H. Yang, R. Yan, H. Chen, C. Zheng, D.H. Lee, D.T. Liang, In-Depth Investigation of Biomass Pyrolysis
610   Based on Three Major Components: Hemicellulose, Cellulose and Lignin, Energy & Fuels. 20 (2006) 388–
611   393. doi:10.1021/ef0580117.

612   [33]   C. Fushimi, K. Araki, Y. Yamaguchi, A. Tsutsumi, Effect of heating rate on steam gasification of biomass.
613   2. Thermogravimetric-mass spectrometric (TG-MS) analysis of gas evolution, Ind. Eng. Chem. Res. 42
614   (2003) 3929–3936. doi:10.1021/ie0300575.

615   [34]   H. Yang, R. Yan, H. Chen, D.H. Lee, C. Zheng, Characteristics of hemicellulose, cellulose and lignin
616   pyrolysis, Fuel. 86 (2007) 1781–1788. doi:10.1016/j.fuel.2006.12.013.

617   [35]   S. Wang, G. Dai, H. Yang, Z. Luo, Lignocellulosic biomass pyrolysis mechanism: A state-of-the-art review,
618   Prog. Energy Combust. Sci. 62 (2017) 33–86. doi:10.1016/j.pecs.2017.05.004.

619   [36]   R.K. Sharma, J.B. Wooten, V.L. Baliga, X. Lin, W.G. Chan, M.R. Hajaligol, Characterization of chars from
620   pyrolysis of lignin, Fuel. 83 (2004) 1469–1482. doi:10.1016/j.fuel.2003.11.015.

621   [37]   H. Lu, E. Ip, J. Scott, P. Foster, M. Vickers, L.L. Baxter, Effects of particle shape and size on
622   devolatilization of biomass particle, Fuel. 89 (2010) 1156–1168. doi:10.1016/j.fuel.2008.10.023.

623   [38]   J. Shen, X.S. Wang, M. Garcia-Perez, D. Mourant, M.J. Rhodes, C.Z. Li, Effects of particle size on the fast
624   pyrolysis of oil mallee woody biomass, Fuel. 88 (2009) 1810–1817. doi:10.1016/j.fuel.2009.05.001.

625   [39]   F. Ronsse, S. van Hecke, D. Dickinson, W. Prins, Production and characterization of slow pyrolysis biochar:
626   Influence of feedstock type and pyrolysis conditions, GCB Bioenergy. 5 (2013) 104–115.
627   doi:10.1111/gcbb.12018.

628   [40]   W.T. Tsai, S.C. Liu, Effect of temperature on thermochemical property and true density of torrefied coffee
629   residue, J. Anal. Appl. Pyrolysis. 102 (2013) 47–52. doi:10.1016/j.jaap.2013.04.003.

630 [41] T. Mekonnen, P. Mussone, K. Alemaskin, L. Sopkow, J. Wolodko, P. Choi, D. Bressler, Biocomposites
631   from hydrolyzed waste proteinaceous biomass: mechanical, thermal and moisture absorption performances,
632   J. Mater. Chem. A. 1 (2013) 13186. doi:10.1039/c3ta13560h.

633 [42] T.J. Haas, M.R. Nimlos, B.S. Donohoe, Real-Time and Post-reaction Microscopic Structural Analysis of
634   Biomass Undergoing Pyrolysis, Energy & Fuels. 23 (2009) 3810–3817. doi:10.1021/ef900201b.

635 [43] B. Chen, D. Zhou, L. ZHU, Transitional Adsorption and Partition of Nonpolar and Polar Aromatic
636   Contaminants by Biochars of Pine Needles with Different Pyrolytic Temperatures, Environ. Sci. Technol.
637   42 (2008) 5137–5143. doi:10.1021/es8002684.

638 [44] A. Pimchuai, A. Dutta, P. Basu, Torrefaction of agriculture residue to enhance combustible properties,
639   Energy and Fuels. 24 (2010) 4638–4645. doi:10.1021/ef901168f.

640 [45] P.A. Della Rocca, E.G. Cerrella, P.R. Bonelli, A.L. Cukierman, Pyrolysis of hardwoods residues: On
641   kinetics and chars characterization, Biomass and Bioenergy. 16 (1999) 79–88. doi:10.1016/S0961-
642   9534(98)00067-1.

643 [46] R. Pietrzak, Sawdust pellets from coniferous species as adsorbents for NO2removal, Bioresour. Technol.
644   101 (2010) 907–913. doi:10.1016/j.biortech.2009.09.017.

645 [47] B. Shrestha, Y. Le Brech, T. Ghislain, S. Leclerc, V. Carré, F. Aubriet, S. Hoppe, P. Marchal, S.
646   Pontvianne, N. Brosse, A. Dufour, A Multitechnique Characterization of Lignin Softening and Pyrolysis,
647   ACS Sustain. Chem. Eng. 5 (2017) 6940–6949. doi:10.1021/acssuschemeng.7b01130.

648 [48] T. Vuolio, Improvement potential of primary hot metal desulphurization, University of Oulu, 2017.

649 [49] H. Lu, X. Guo, X. Gong, X. Cong, K. Liu, H. Qi, Experimental study on aerated discharge of pulverized
650   coal, Chem. Eng. Sci. 71 (2012) 438–448. doi:10.1016/j.ces.2011.11.006.

651 [50] O. Mattila, K. Keski--Ruismäki, T. Paananen, From Oil to Coal Injection – Experiences and First
652   Development Steps, in: 2 Nd ISIJ-VDEh-Jernkontoret Jt. Symp., Stockholm, Sweden, n.d.: pp. 166–177.

653 [51] S. Rodrigues, I. Suárez-Ruiz, M. Marques, I. Camean, D. Flores, Microstructural evolution of high
654   temperature treated anthracites of different rank, Int. J. Coal Geol. 87 (2011) 204–211.
655   doi:10.1016/j.coal.2011.06.009.

656 [52] C.C.T. Barbieri, E. Osório, A.C.F. Vilela, Combustibility and reactivity of coal blends and charcoal fines
657   aiming use in ironmaking, Mater. Res. 19 (2016) 594–601. doi:10.1590/1980-5373-MR-2015-0705.

658 [53] Q. Li, C. Zhao, X. Chen, W. Wu, Y. Li, Comparison of pulverized coal combustion in air and in O2/CO2
659   mixtures by thermo-gravimetric analysis, J. Anal. Appl. Pyrolysis. 85 (2009) 521–528.
660   doi:10.1016/j.jaap.2008.10.018.

661 [54] T. Abbas, P. Costen, N.H. Kandamby, F.C. Lockwood, J.J. Ou, The influence of burner injection mode on
662   pulverized coal and biomass co-fired flames, Combust. Flame. 99 (1994) 617–625.
663   doi:https://doi.org/10.1016/0010-2180(94)90055-8.

664

Highlights:

- First study on pyrolysis of lignin recovered from wood-based ethanol production.
- Pyrolyzed lignin has high mass/energy yield up to 73/89% and HHV up to 34.31 MJ/kg.
- Effect of temperature on Physico-chemical characteristics of chars investigated.
- Best lignin char to substitute coal in BF injection obtained in pyrolysis at 500 ^{o}C.
- Pyrolysis in lower temperatures resulted in high combustibility and low water uptake